

Omental Vascularized Lymph Node Flap: A Radiographic Analysis

Julia A. Cook, MD¹ Sarah E. Sasor, MD¹ Sunil S. Tholpady, MD, PhD^{1,2} Michael W. Chu, MD³

¹Division of Plastic and Reconstructive Surgery, Department of Surgery, Indiana University School of Medicine, Indianapolis, Indiana

²Division of Plastic and Reconstructive Surgery, R.L. Roudebush Veterans Administration Medical Center, Indianapolis, Indiana

³Division of Plastic and Reconstructive Surgery, Kaiser Permanente West Los Angeles Medical Center, Los Angeles, California

Address for correspondence Julia A. Cook, MD, Division of Plastic and Reconstructive Surgery, Department of Surgery, Indiana University School of Medicine, 545 Barnhill Drive, #232, Indianapolis, IN 46202 (e-mail: juacook@gmail.com).

J Reconstr Microsurg 2018;34:472–477.

Abstract

Background Vascularized lymph node transfer is an increasingly popular option for the treatment of lymphedema. The omental donor site is advantageous for its copious soft tissue, well-defined collateral circulation, and large number of available nodes, without the risk of iatrogenic lymphedema. The purpose of this study is to define the anatomy of the omental flap in the context of vascularized lymph node harvest.

Methods Consecutive abdominal computed tomography angiography (CTA) images performed at a single institution over a 1-year period were reviewed. Right gastroepiploic artery (RGEA) length, artery caliber, lymph node size, and lymph node location in relation to the artery were recorded. A two-tailed Z-test was used to compare means. A Gaussian Mixture Model confirmed by normalized entropy criterion was used to calculate three-dimensional lymph node cluster locations along the RGEA.

Results In total, 156 CTA images met inclusion criteria. The RGEA caliber at its origin was significantly larger in males compared with females ($p < 0.001$). An average of 3.1 (1.7) lymph nodes were present per patient. There was no significant gender difference in the number of lymph nodes identified. Average lymph node size was significantly larger in males (4.9 [1.9] × 3.3 [0.6] mm in males vs. 4.5 [1.5] × 3.1 [0.5] mm in females; $p < 0.001$). Three distinct anatomical variations of the RGEA course were noted, each with a distinct lymph node clustering pattern. Total lymph node number and size did not differ among anatomical subgroups.

Conclusion The omentum is a reliable lymph node donor site with consistent anatomy. This study serves as an aid in preoperative planning for vascularized lymph node transfer using the omental flap.

Keywords

- ▶ omental flap
- ▶ vascularized lymph node transfer
- ▶ lymphedema

Lymphedema is a chronic, debilitating condition that affects millions of people worldwide. The prevalence of lymphedema is expected to increase as cancer treatments become more advanced and survivorship improves. The true incidence of lymphedema is difficult to determine because definitions, diagnoses, and duration of follow-up vary. This is seen in breast cancer related lymphedema, as the reported

rate varies from 4 to 56%.^{1–12} Lymphedema patients report lower quality of life, frequent episodes of cellulitis, lymphangitis, and decreased extremity range of motion.^{13,14}

Vascularized lymph node transfer (VLNT) is a promising surgical treatment option to treat lymphedema. Donor sites such as the submental, supraclavicular, axillary, and groin nodes have been described, but these sites have the potential

received

December 1, 2017

accepted after revision

January 18, 2018

published online

April 16, 2018

Copyright © 2018 by Thieme Medical Publishers, Inc., 333 Seventh Avenue, New York, NY 10001, USA.
Tel: +1(212) 584-4662.

DOI <https://doi.org/10.1055/s-0038-1642637>.
ISSN 0743-684X.

to cause iatrogenic lymphedema^{13,15–18} and may have limited soft tissue availability.¹⁹ The omentum is recognized for its rich reservoir of lymphatic tissue,^{20,21} redundant collateral circulation,^{22–24} and copious soft tissue availability.²³ The omental lymph nodes have therefore been investigated as a potential donor site, and to date, there are no reported cases of iatrogenic donor site lymphedema.^{20,25} The purpose of our study is to characterize the anatomy, quantity and location of lymph nodes, and vascular anatomy of the omental lymph node flap. This characterization can be used in preoperative planning for patients undergoing VLNT.

Methods

An institutional review board approved retrospective analysis of consecutive abdominal computed tomography angiography (CTA) studies performed at a single institution over an 8-month period was completed. Indications for CTA imaging included evaluation of vascular anomalies, abdominal masses, epigastric pain, and kidney donation potential. Patients with a history of previous abdominal surgery, cirrhosis with portal hypertension, omental disease, active gastrointestinal bleeding, poor right gastroepiploic arterial phase timing, dissection of the celiac artery, thrombosis of the celiac artery, and stenosis of the celiac artery were excluded. Studies with excess artifact or degradation due to patient motion or position, and studies with incomplete imaging of the abdominal wall were also excluded.

The right gastroepiploic artery (RGEA) was identified and its course was analyzed and categorized into subgroups, defined by the course of the RGEA from its origin to termination. The origin was defined at the point of bifurcation of the gastroduodenal artery into the superior pancreaticoduodenal artery and RGEA. Artery termination was defined at the point where the RGEA passes the splenic artery. Additional anatomical measurements included the RGEA pedicle length, RGEA and right gastroepiploic vein (RGEV) intraluminal caliber at the gastroepiploic origin, lymph node length and width, and three-dimensional distance of each lymph node from the gastroepiploic origin using both coronal (►Fig. 1) and axial (►Fig. 2) views. Each variable was measured three times and

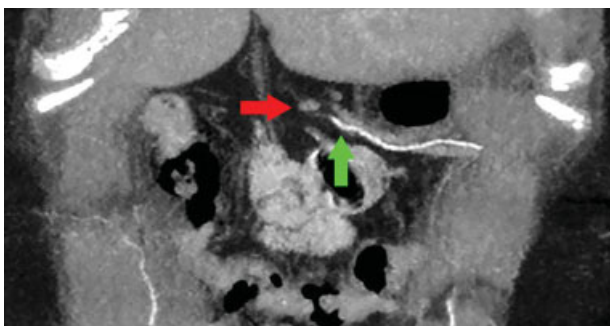


Fig. 1 Lymph node located along the right gastroepiploic artery on coronal computed tomography (CT) angiography abdomen imaging. Horizontal arrow is indicative of gastroepiploic lymph node. Vertical arrow is indicative of the right gastroepiploic artery and vein.



Fig. 2 Lymph node located along the right gastroepiploic artery on axial computed tomography (CT) angiography imaging of the abdomen. Arrow is indicative of gastroepiploic lymph node.

averaged by two independent reviewers; measurements with a range of ≥ 0.5 mm were repeated.

All scans were performed in a 64-detector scanner (Aquilion 64, Toshiba Medical Systems, Otawara, Japan) using standard CTA imaging protocols. A weight-based bolus of iodinated contrast agent was administered intravenously, and images were taken at 0.5-mm intervals. Reconstructed axial images were processed to create multiplanar reconstructions (Synapse version 4.3, Fujifilm, Tokyo, Japan).

Statistical Analysis

All measurements were reported as means, and a two-tailed Z-test was used to compare results. Pearson correlation and simple linear regression analyses for colinearity were conducted to predict intraluminal diameter in relation to vascular comorbidities (XLSTAT version 2017.5, Addinsoft, New York, NY). A Gaussian mixture model was trained for each pedicle class. The expectation–management (EM) algorithm was used to estimate the mean vectors, covariance matrices, and prior probabilities. Cohen's kappa (κ) coefficient was used to measure interrater agreement between the two independent reviewers. Statistical significance was set at a p -value of ≤ 0.05 .

Results

Composite Data

A total of 237 consecutive patients were evaluated and 156 (65.8%) met inclusion criteria. Of the included patients, 88 (56.4%) were male. The average age of patients was 60.7 (16.1) years old and did not differ significantly between males and females (62.6 [16] and 58.3 [15.9] years, respectively; $p = 0.09$). Mean body mass index (BMI) was 29.3 (6.5) kg/m², with no significant difference between males (29.6 [5.9] kg/m²) and females (28.8 [7.2] kg/m²; $p = 0.41$).

There was a high degree of agreement between the two reviewers, $\kappa = 0.84$ (95% confidence interval: 0.62–0.96; $p < 0.006$), as seen in ►Table 1. The right gastroepiploic pedicle length was 192.2 (39.7) mm long with no significant difference in length between males and females (196.3 [41.1]

Table 1 Cohen's kappa: inter- and intra-rater reliability

	Intrater reliability	Interrater reliability
RGEA pedicle length	0.90	0.85
RGEA caliber	0.91	0.80
RGEV caliber	0.94	0.86
Node position, x	0.89	0.88
Node position, y	0.95	0.89
Node position, z	0.92	0.91
Node length	0.91	0.92
Node width	0.94	0.90

Abbreviations: RGEA, right gastroepiploic artery; RGEV, right gastroepiploic vein.

and 186.8 [37.6] mm, respectively; $p = 0.13$). The RGEA had a significantly larger caliber in males as compared with females (3.2 [0.5] and 2.9 [0.5] mm, respectively; $p < 0.001$). The RGEV also had a significantly larger caliber in males (4.2 [0.7] and 3.7 [0.4] mm; $p < 0.001$). An average of 3.1 (1.7) lymph nodes were present per study. Average lymph node size was significantly larger in males (4.9 [1.9] × 3.3 [0.6] mm in males vs. 4.5 [1.5] × 3.1 [0.5] mm in females; $p < 0.001$). There was no significant gender difference in the number of lymph nodes identified (3 [1.7] in men and 3.2 [1.6] in women; $p = 0.37$).

Cook–Chu Right Gastroepiploic Artery Classification

The RGEA had the following three anatomical variants in the study population:

- Class I (47.4%): following the bifurcation of the gastroduodenal artery into the RGEA and the superior pancreaticoduodenal artery, the RGEA travels ≥ 10 mm right lateral toward the liver prior to coursing left lateral to supply the greater curvature of the stomach (→ Fig. 3).

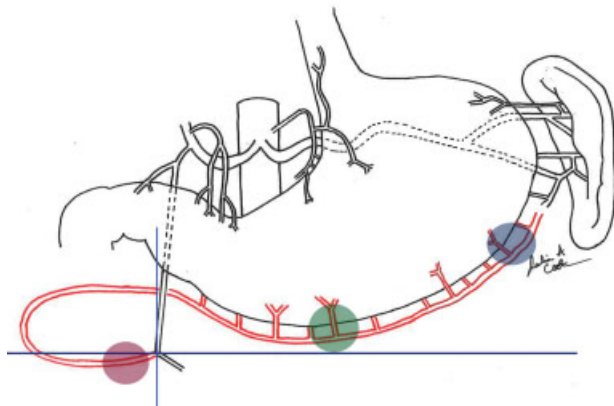


Fig. 3 Class I right gastroepiploic artery (RGEA). Following gastroduodenal artery bifurcation, the RGEA travels ≥ 10 mm right lateral toward liver prior to coursing left lateral to supply greater curvature of the stomach. Inferior vessel is indicative of the right gastroepiploic artery. Left circle: group 1 lymph node cluster location. Middle circle: group 2 lymph node cluster location. Right circle: group 3 lymph node cluster location.

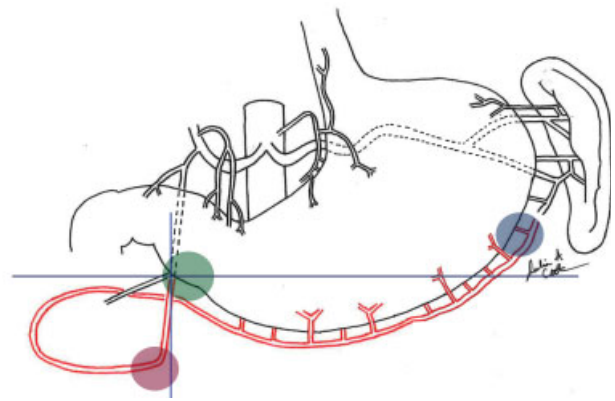


Fig. 4 Class II right gastroepiploic artery (RGEA). Following gastroduodenal artery bifurcation, the RGEA travels ≥ 10 mm caudally prior to coursing toward the greater curvature of stomach. Inferior vessel is indicative of the right gastroepiploic artery. Left circle: group 1 lymph node cluster location. Middle circle: group 2 lymph node cluster location. Right circle: group 3 lymph node cluster location.

- Class II (30.8%): following the bifurcation of the gastroduodenal artery, the RGEA courses ≥ 10 mm caudally prior to coursing toward the greater curvature of the stomach (→ Fig. 4).
- Class III (21.8%): following the bifurcation of the gastroduodenal artery, the RGEA immediately courses toward the greater curvature of the stomach (→ Fig. 5).

Class I anatomy was most common and present in 43 males and 31 females. Average RGEA pedicle length was 199.6 (34.6) mm and did not differ between males and females (200.6 [35.5] mm and 198.2 [33.7]; $p = 0.80$). RGEA caliber was larger in males (3.1 [0.5] mm) as compared with females (2.9 [0.5] mm; $p = 0.05$). Mean RGEV diameter was 4 (0.6) mm and did not significantly differ between males (4.1 [0.6] mm) and females (3.9 [0.7] mm; $p = 0.11$). Females (3.8 [1.8] mm) had significantly more lymph nodes

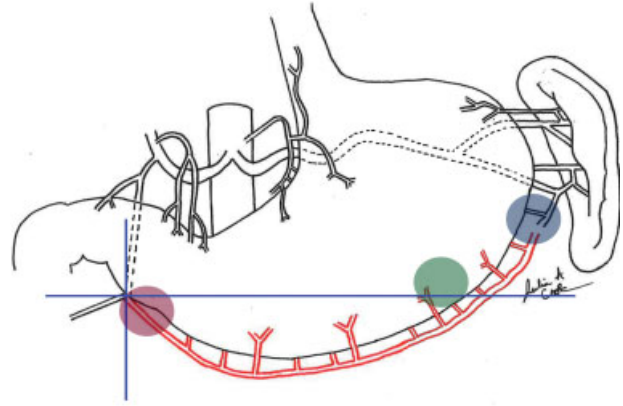


Fig. 5 Class III right gastroepiploic artery. Following gastroduodenal artery bifurcation, the artery immediately courses toward the greater curvature of the stomach. Inferior vessel is indicative of the right gastroepiploic artery. Left circle: group 1 lymph node cluster location. Middle circle: group 2 lymph node cluster location. Right circle: group 3 lymph node cluster location.

than males (2.9 [1.4] mm; $p = 0.03$). One study examined had no identifiable lymph nodes. Lymph node length and width was on average 4.7 (1.3) \times 3.2 (0.7) mm and did not differ significantly between males (4.9 [1.4] \times 3.2 [0.7] mm) and females (4.6 [1.2] \times 3.1 [0.7] mm; $p = 0.07$ and 0.17).

Class II anatomy was found in 28 males and 19 females; 147 lymph nodes were identified. One study had no identifiable lymph nodes. The average pedicle length was 202.4 (43.6) mm and did not differ significantly between males (206.5 [48.3] mm) and females (196.8 [36.6] mm; $p = 0.43$). RGEA and RGEV calibers were significantly large in males (3.3 [0.6] and 2.8 [0.6] mm, respectively) compared with females (2.8 [0.4] and 3.6 [0.6] mm; $p < 0.001$ and < 0.001). Number of lymph nodes did not differ significantly between males and females (3.1 [2.3] and 3 [1.4], respectively; $p = 0.79$). Lymph node length and width was larger in males (5 [1.3] \times 3.5 [0.7] mm) as compared with females (4.5 [1.3] \times 3.1 [0.8]; $p = 0.02$ and 0.01).

Class III anatomy was seen in 17 males and 17 females; 90 lymph nodes were identified. One study meeting inclusion criteria demonstrated no lymph nodes. The average pedicle length was 161.5 (28.6) mm and did not differ significantly between males (170.1 [29.6] mm) and females (164.2 [26.4] mm; $p = 0.11$). The RGEA had an average caliber of 2.9 (0.5) mm without significant difference between males (2.9 [0.5] mm) and females (2.9 [0.5] mm; $p = 0.890$). The RGEV had an average caliber of 3.8 (0.7) mm and did not demonstrate a significant difference between males (4 [0.8] mm) and females (3.6 [0.5] mm; $p = 0.16$). An average of 2.7 (1.4) lymph nodes were identified per pedicle with no significant difference between males (2.8 [1.4] and females (2.5 [1.4]). Average lymph node length and width was 4.8 (1.4) \times 3.2 (0.8) mm and did not differ significantly between males (4.9 [1.6] \times 3.3 [0.8] mm) and females (4.6 [1] \times 3.1 [0.6] mm; $p = 0.22$ and 0.12).

For each pedicle class, 20 iterations of the EM algorithm were enough to converge. Clustering analysis was performed for the three-dimensional location of each lymph node for each pedicle class.²⁶ Each RGEA class had three areas of lymph node clustering found at distinct, three-dimensional locations along the artery (**→ Figs. 3–5, → Table 2**).

Vascular Comorbidities

Vascular comorbidities were common in this cohort: 61% had hypertension, 44% had hyperlipidemia, 28% had coronary artery disease, 18% had diabetes mellitus, 11% had peripheral vascular disease, and 6% had congestive heart failure. After controlling for vascular comorbidities, obese patients (BMI ≥ 30 kg/m²) demonstrated significantly greater arterial caliber (3.2 [0.27] mm) compared with nonobese individuals (2.8 [0.17] mm; $p < 0.001$). The RGEV also demonstrated significantly larger caliber in obese individuals (4.1 [0.5] mm vs. 3.7 [0.3] mm; $p < 0.001$). Linear regression analysis also demonstrated a positive correlation between BMI and arterial (RGEA caliber = 2.42 + 0.02 [BMI], $R^2 = 0.07$, $F = 11.4$, $p < 0.001$) and venous caliber (RGEV caliber = 3.1 + 0.03 [BMI], $R^2 = 0.08$, $F = 12.7$, $p < 0.001$). Other vascular comorbidities did not affect arterial or venous caliber.

Total number of lymph nodes per pedicle did not vary with the presence of vascular comorbidities; however, lymph node size was larger in obese patients compared to patients with a normal BMI (4.1 [0.7] \times 3.2 [0.5] mm, $p < 0.001$, vs. 3.7 [0.6] \times 2.8 [0.4] mm, $p < 0.001$). Other vascular comorbidities did not affect lymph node size.

Discussion

The omental lymph node flap is an ideal donor site due to the low risk of iatrogenic lymphedema.²⁷ First described in 1967 by Goldsmith et al,²⁸ the flap has been slow to gain popularity due to concerns regarding an open abdominal procedure.^{29–31} Laparoscopic harvest techniques have renewed interest in this donor site for VLNT; scarring is minimized³² and donor site morbidity is reduced.³³

The omental flap comprises two dominant pedicles, the right and left gastroepiploic vessels.²⁴ The RGEA is preferred because it is larger, has more epiploic branches, and is easily accessible through a laparoscopic approach.^{20,21,33,34} The omentum consists of a vast network of lymphoreticular bodies that drain into the lymphatic collecting system along the right gastroepiploic pedicle and should be preserved during dissection.^{20,21}

Table 2 Three-dimensional coordinates, lymph node dimension, and proportion of lymph nodes per cluster for each pedicle class

		Group 1	Group 2	Group 3
Class I	Coordinates (x, y, z), mm	(−8.1, −3.2, 16.2)	(25, 8.2, 62.1)	(79.3, 33.2, 43)
	LN dimension, mean (SD), mm	4.5 (1.1) \times 3.3 (0.9)	4.7 (1) \times 3.1 (0.9)	5.2 (1.1) \times 3.2 (1)
	Proportion	0.69	0.17	0.14
Class II	Coordinates (x, y, z), mm	(−2.2, −18.5, 16.2)	(4.8, 1, 71.8)	(70.1, 6.1, 29.4)
	LN dimension, mean (SD), mm	4.9 (0.8) \times 3.3 (0.8)	4.7 (0.9) \times 3.3 (0.8)	4.3 (1) \times 3.2 (0.8)
	Proportion	0.68	0.11	0.21
Class III	Coordinates (x, y, z), mm	(6.8, −2.2, 11)	(52, 10, 31.6)	(63, 56.4, 56)
	LN dimension, mean (SD), mm	4.9 (0.9) \times 3.3 (0.7)	4.8 (0.8) \times 3.3 (0.9)	4.7 (1) \times 3.8 (0.9)
	Proportion	0.59	0.26	0.15

Abbreviations: LN, lymph node; SD, standard deviation.

This study is the first to describe a classification system of the RGEA and its associated lymph nodes. The study findings can be helpful in preoperative planning by understanding anatomical differences. Current literature suggests that a vascularized flap containing two or three lymph nodes is sufficient for improvement of lymphedema.^{15,35} Our results demonstrate that all three classes of right gastroepiploic anatomy can supply sufficient lymph nodes for a successful VLNT. If a surgeon's preference is to transfer more than two lymph nodes, patients with class III anatomy may require further omental dissection.

Our study supports previous literature suggesting that obese patients have larger caliber vessels.^{36–38} Larger vessel caliber makes microanastomoses easier and more successful.^{39,40} This finding supports existing data that microsurgery in obese patients is feasible and safe, and increased BMI may have an improved effect on anastomotic patency outcomes.

Our study is the first to demonstrate a significant relationship between lymph node size and obesity. The clinical implications of this relationship are not yet known.

This study is limited by its retrospective nature, lack of surgical correlation to radiographic findings, and the inherent limits of CT angiography. CT images comprise a series of square data points called voxels. Each voxel has a numerical value representing the calculated density of a structure measured in Hounsfield units (HUs).⁴¹ If a voxel contains two areas with different HUs, the voxel is assigned the average as different densities within a voxel cannot be separated. Smaller voxels are required to increase precision, but smaller voxels are more sensitive to background noise and can distort the vascular lumen.⁴² In angiographic imaging, postprocessing manipulates voxels by discarding non-vascular data to enhance vascular structures and requires high contrast between vascular and nonvascular structures.⁴³ Despite these limitations, CTA is a useful radiographic study to assess vasculature in reconstructive settings. The criterion standard is invasive angiography, but CTA sensitivity and specificity approach 90% and avoids the risks of arterial puncture, hematoma, and infection.⁴⁴ In addition, CTA provides axial images that allow for direct visualization of vessel lumen and has accuracy in measuring perforator vessel size greater than 0.3 mm in diameter.⁴⁵

This study does not advocate for routine, preoperative CT scans, and its results must be interpreted carefully. However, the study has many interesting findings that can be useful in counseling and preoperative planning for vascularized omental lymph node transfers. Finally, CTA has demonstrated complete concordance between radiological and surgical findings.^{46–50}

Conclusion

An ideal lymph node donor site would have a sufficient number of donor nodes, a vascular pedicle of adequate length and caliber, and low risk of donor site lymphedema. The results of this study indicate that the omental lymph node flap can satisfy these requirements. Understanding lymph node clustering along the RGEA is helpful in preoperative planning for this donor site. Future studies should confirm

these findings using lymphoscintigraphy or indocyanine green fluorescence.

Conflict of Interest

None.

References

- Petrek JA, Pressman PI, Smith RA. Lymphedema: current issues in research and management. *CA Cancer J Clin* 2000;50(05):292–307, quiz 308–311
- Beaulac SM, McNair LA, Scott TE, LaMorte WW, Kavanah MT. Lymphedema and quality of life in survivors of early-stage breast cancer. *Arch Surg* 2002;137(11):1253–1257
- Coen JJ, Taghian AG, Kachnic LA, Assaad SI, Powell SN. Risk of lymphedema after regional nodal irradiation with breast conservation therapy. *Int J Radiat Oncol Biol Phys* 2003;55(05):1209–1215
- Golshan M, Martin WJ, Dowlatshahi K. Sentinel lymph node biopsy lowers the rate of lymphedema when compared with standard axillary lymph node dissection. *Am Surg* 2003;69(03):209–211, discussion 212
- Herd-Smith A, Russo A, Muraca MG, Del Turco MR, Cardona G. Prognostic factors for lymphedema after primary treatment of breast carcinoma. *Cancer* 2001;92(07):1783–1787
- Kosir MA, Rymal C, Koppolu P, et al. Surgical outcomes after breast cancer surgery: measuring acute lymphedema. *J Surg Res* 2001;95(02):147–151
- Meric F, Buchholz TA, Mirza NQ, et al. Long-term complications associated with breast-conservation surgery and radiotherapy. *Ann Surg Oncol* 2002;9(06):543–549
- Paskett ED, Naughton MJ, McCoy TP, Case LD, Abbott JM. The epidemiology of arm and hand swelling in premenopausal breast cancer survivors. *Cancer Epidemiol Biomarkers Prev* 2007;16(04):775–782
- Schijven MP, Vingerhoets AJ, Rutten HJ, et al. Comparison of morbidity between axillary lymph node dissection and sentinel node biopsy. *Eur J Surg Oncol* 2003;29(04):341–350
- Schrenk P, Rieger R, Shamiyeh A, Wayand W. Morbidity following sentinel lymph node biopsy versus axillary lymph node dissection for patients with breast carcinoma. *Cancer* 2000;88(03):608–614
- Sener SF, Winchester DJ, Martz CH, et al. Lymphedema after sentinel lymphadenectomy for breast carcinoma. *Cancer* 2001;92(04):748–752
- Tengrup I, Tennvall-Nittby L, Christiansson I, Laurin M. Arm morbidity after breast-conserving therapy for breast cancer. *Acta Oncol* 2000;39(03):393–397
- Cheng MH, Chen SC, Henry SL, Tan BK, Lin MC, Huang JJ. Vascularized groin lymph node flap transfer for postmastectomy upper limb lymphedema: flap anatomy, recipient sites, and outcomes. *Plast Reconstr Surg* 2013;131(06):1286–1298
- Shih YC, Xu Y, Cormier JN, et al. Incidence, treatment costs, and complications of lymphedema after breast cancer among women of working age: a 2-year follow-up study. *J Clin Oncol* 2009;27(12):2007–2014
- Cheng MH, Huang JJ, Nguyen DH, et al. A novel approach to the treatment of lower extremity lymphedema by transferring a vascularized submental lymph node flap to the ankle. *Gynecol Oncol* 2012;126(01):93–98
- Cheng MH, Huang JJ, Wu CW, et al. The mechanism of vascularized lymph node transfer for lymphedema: natural lymphaticovenous drainage. *Plast Reconstr Surg* 2014;133(02):192e–198e
- Raju A, Chang DW. Vascularized lymph node transfer for treatment of lymphedema: a comprehensive literature review. *Ann Surg* 2015;261(05):1013–1023
- Althubaiti GA, Crosby MA, Chang DW. Vascularized supraclavicular lymph node transfer for lower extremity lymphedema treatment. *Plast Reconstr Surg* 2013;131(01):133e–135e

- 19 Ozturk CN, Ozturk C, Glasgow M, et al. Free vascularized lymph node transfer for treatment of lymphedema: a systematic evidence based review. *J Plast Reconstr Aesthet Surg* 2016;69(09):1234–1247
- 20 Nguyen AT, Suami H. Laparoscopic free omental lymphatic flap for the treatment of lymphedema. *Plast Reconstr Surg* 2015;136(01):114–118
- 21 Liebermann-Meffert D. The greater omentum. *Anatomy, embryology, and surgical applications. Surg Clin North Am* 2000;80(01):275–293, xii
- 22 Lasso JM, Pinilla C, Castellano M. New refinements in greater omentum free flap transfer for severe secondary lymphedema surgical treatment. *Plast Reconstr Surg Glob Open* 2015;3(05):e387
- 23 Losken A, Carlson GW, Culbertson JH, et al. Omental free flap reconstruction in complex head and neck deformities. *Head Neck* 2002;24(04):326–331
- 24 Boulton BJF. S. The technique of omentum harvest for intrathoracic use. *Oper Tech Thorac Cardiovasc Surg* 2010;15(01):53–60
- 25 Benoit L, Boichot C, Cheynel N, et al. Preventing lymphedema and morbidity with an omentum flap after ilioinguinal lymph node dissection. *Ann Surg Oncol* 2005;12(10):793–799
- 26 Fraley C, Raftery AE. How many clusters? Which clustering method? Answers via model-based cluster analysis. *Comput J* 1998;41(08):578–588
- 27 Chu YY, Allen RJ Jr, Wu TJ, Cheng MH. Greater omental lymph node flap for upper limb lymphedema with lymph nodes-depleted patient. *Plast Reconstr Surg Glob Open* 2017;5(04):e1288
- 28 Goldsmith HS, De los Santos R, Beattie EJ Jr. Relief of chronic lymphedema by omental transposition. *Ann Surg* 1967;166(04):573–585
- 29 van Wingerden JJ, Coret ME, van Nieuwenhoven CA, Totté ER. The laparoscopically harvested omental flap for deep sternal wound infection. *Eur J Cardiothorac Surg* 2010;37(01):87–92
- 30 El Gamel A, Yonan NA, Hassan R, et al. Treatment of mediastinitis: early modified Robicsek closure and pectoralis major advancement flaps. *Ann Thorac Surg* 1998;65(01):41–46, discussion 46–47
- 31 Hakelius L. Fatal complication after use of the greater omentum for reconstruction of the chest wall: case report. *Plast Reconstr Surg* 1978;62(05):796–797
- 32 Salameh JR, Chock DA, Gonzalez JJ, Koneru S, Glass JL, Franklin ME Jr. Laparoscopic harvest of omental flaps for reconstruction of complex mediastinal wounds. *JSLs* 2003;7(04):317–322
- 33 Zaha H, Inamine S, Naito T, Nomura H. Laparoscopically harvested omental flap for immediate breast reconstruction. *Am J Surg* 2006;192(04):556–558
- 34 Saltz R, Stowers R, Smith M, Gadacz TR. Laparoscopically harvested omental free flap to cover a large soft tissue defect. *Ann Surg* 1993;217(05):542–546, discussion 546–547
- 35 Gharb BB, Rampazzo A, Spanio di Spilimbergo S, Xu ES, Chung KP, Chen HC. Vascularized lymph node transfer based on the hilar perforators improves the outcome in upper limb lymphedema. *Ann Plast Surg* 2011;67(06):589–593
- 36 Cook JA, Tholpady SS, Momeni A, Chu MW. Predictors of internal mammary vessel diameter: a computed tomographic angiography-assisted anatomic analysis. *J Plast Reconstr Aesthet Surg* 2016;69(10):1340–1348
- 37 Gusenoff JA, Coon D, De La Cruz C, Rubin JP. Superficial inferior epigastric vessels in the massive weight loss population: implications for breast reconstruction. *Plast Reconstr Surg* 2008;122(06):1621–1626
- 38 Hanssen H, Siegrist M, Neidig M, et al. Retinal vessel diameter, obesity and metabolic risk factors in school children (JuvenTUM 3). *Atherosclerosis* 2012;221(01):242–248
- 39 Broer PN, Weichman KE, Tanna N, et al. Venous coupler size in autologous breast reconstruction—does it matter? *Microsurgery* 2013;33(07):514–518
- 40 Moran SL, Serletti JM. Outcome comparison between free and pedicled TRAM flap breast reconstruction in the obese patient. *Plast Reconstr Surg* 2001;108(07):1954–1960
- 41 Langheinrich AC, Kampschulte M, Crössmann C, et al. Role of computed tomography voxel size in detection and discrimination of calcium and iron deposits in atherosclerotic human coronary artery specimens. *J Comput Assist Tomogr* 2009;33(04):517–522
- 42 Fansa H, Schirmer S, Cervelli A, Gehl HB. Computed tomographic angiography imaging and clinical implications of internal mammary artery perforator vessels as recipient vessels in autologous breast reconstruction. *Ann Plast Surg* 2013;71(05):533–537
- 43 Gonzalez RG, Hirsch JA, Koroshetz WJ. *Acute Ischemic Stroke: Imaging and Intervention*. New York, NY: Springer; 2011
- 44 Tavakol M, Ashraf S, Brener SJ. Risks and complications of coronary angiography: a comprehensive review. *Glob J Health Sci* 2012;4(01):65–93
- 45 Rozen WM, Stella DL, Bowden J, Taylor GI, Ashton MW. Advances in the pre-operative planning of deep inferior epigastric artery perforator flaps: magnetic resonance angiography. *Microsurgery* 2009;29(02):119–123
- 46 Murray AC, Rozen WM, Alonso-Burgos A, Ashton MW, Garcia-Tutor E, Whitaker IS. The anatomy and variations of the internal thoracic (internal mammary) artery and implications in autologous breast reconstruction: clinical anatomical study and literature review. *Surg Radiol Anat* 2012;34(02):159–165
- 47 Kim H, Lim SY, Pyon JK, Bang SI, Oh KS, Mun GH. Preoperative computed tomographic angiography of both donor and recipient sites for microsurgical breast reconstruction. *Plast Reconstr Surg* 2012;130(01):11e–20e
- 48 Smit JM, Klein S, Werker PM. An overview of methods for vascular mapping in the planning of free flaps. *J Plast Reconstr Aesthet Surg* 2010;63(09):e674–e682
- 49 Rozen WM, Stella DL, Phillips TJ, Ashton MW, Corlett RJ, Taylor GI. Magnetic resonance angiography in the preoperative planning of DIEA perforator flaps. *Plast Reconstr Surg* 2008;122(06):222e–223e
- 50 Masia J, Clavero JA, Larrañaga JR, Alomar X, Pons G, Serret P. Multidetector-row computed tomography in the planning of abdominal perforator flaps. *J Plast Reconstr Aesthet Surg* 2006;59(06):594–599